

## N O T I C E

THIS DOCUMENT HAS BEEN REPRODUCED FROM  
MICROFICHE. ALTHOUGH IT IS RECOGNIZED THAT  
CERTAIN PORTIONS ARE ILLEGIBLE, IT IS BEING RELEASED  
IN THE INTEREST OF MAKING AVAILABLE AS MUCH  
INFORMATION AS POSSIBLE



## Technical Memorandum 80628

# L-Band Radar Sensing of Soil Moisture

(NASA-TM-80628) L-BAND RADAR SENSING OF  
SOIL MOISTURE (NASA) 32 p HC A03/MF A01  
CSCL 08M

N80-16404

Unclassified

**A. T. C. Chang, S. Atwater, V. V. Salomonson,  
J. E. Estes, D. S. Simonett, and M. L. Bryan**

JANUARY 1980

National Aeronautics and  
Space Administration

**Goddard Space Flight Center**  
Greenbelt, Maryland 20771



## L-BAND RADAR SENSING OF SOIL MOISTURE

A. T. C. Chang,<sup>1</sup>      S. Atwater,<sup>2</sup>      V. V. Salomonson,<sup>1</sup>

J. E. Estes,<sup>2</sup>      D. S. Simonett,<sup>2</sup>      and M. L. Bryan<sup>3</sup>

<sup>1</sup>Laboratory for Atmospheric Sciences  
Goddard Space Flight Center  
Greenbelt, Maryland

<sup>2</sup>University of California, Santa Barbara  
Santa Barbara, California

<sup>3</sup>Jet Propulsion Laboratory  
Pasadena, California

**Page intentionally left blank**

## L-BAND RADAR SENSING OF SOIL MOISTURE

### ABSTRACT

The objectives of this experiment were to assess the performance of an L-band, 25 cm wavelength imaging synthetic aperture radar for soil moisture determination, and to study the temporal variability of radar returns from a number of agricultural fields. A series of three overflights was accomplished during March 1977 over an agricultural test site in Kern County, California. Soil moisture samples were collected from bare fields at nine sites at depths of 0-2, 2-5, 5-15, and 15-30 cm. These gravimetric measurements were converted to percent of field capacity for correlation to the radar return signal. The initial signal film was optically correlated and scanned to produce image data numbers. These numbers were then converted to relative return power by linear interpolation of the noise power wedge which was introduced in 5 dB steps into the original signal film before and after each data run. Results of correlations between the relative return power and percent of field capacity (FC) demonstrate that the relative return power from this imaging radar system is responsive to the amount of soil moisture in bare fields. The signal returned from dry (15% FC) and wet (130% FC) fields where furrowing is parallel to the radar beam differs by about 10 dB. Problems remain to be resolved before this technique can be operationally employed. First, adequate calibration of the radar system is required to insure comparability of data both from area to area within a single flight and between different flights. In addition, more study is needed of the effect of surface roughness on the SAR return which appears in some cases to mask out differences in relative return power due to soil moisture variation. Lastly, furrow direction in relation to beam direction has a significant effect on radar return and needs more study.

**Page intentionally left blank**

## CONTENTS

	<u>Page</u>
INTRODUCTION . . . . .	1
Background . . . . .	3
Aircraft Data Acquisition and Calibration . . . . .	3
Field Verification . . . . .	11
Results and Analysis . . . . .	17
CONCLUSIONS . . . . .	20
REFERENCES . . . . .	26

## ILLUSTRATIONS

<u>Figure</u>		<u>Page</u>
1	Copus Road Transect, Kern County, California . . .	2
2	Slant Range Relationship for a SAR . . . . .	4
3	Calibration Data for March 24, 1977 Flight . . .	6
4	Calibration Data for March 25, 1977 Flight . . .	7
5	Calibration Data for March 28, 1977 Flight . . .	8
6	SAR Image for March 24, 1977 Flight . . . . .	12
7	SAR Image for March 25, 1977 Flight . . . . .	13
8	SAR Image for March 28, 1977 Flight . . . . .	14
9	Calibration Curve for L-Band SAR (HH) . . . . .	15
10	L-Band (HH) Relative Return Power vs Percent Field Capacity for Different Soil Layers . . . . .	19

TABLES

<u>Table</u>		<u>Page</u>
1	Soil Moisture Ground Truth - March 1977 Percent Soil Moisture Average Percent Soil Moisture . . . . .	21
2	Soil Moisture of Ground Truth - March 1977 Percent of Field Capacity Average Percent of Field Capacity . . . . .	22
3	Field Average Percent Moisture Content by Weight. .	23
4	Field Average Percent of Field Capacity . . . . .	24
5	Field Averaged 0-2 cm Percent Moisture Content, Field Capacity and SAR Relative Return Power . . .	25

## INTRODUCTION

In recent years a substantial research program funded by NASA has begun to develop remote sensing techniques for the determination of soil moisture content. Presently this research effort is being driven by potential applications in the areas of hydrology, agriculture, weather and climate. In hydrology, surface runoff after a rainstorm is an important factor in the control and management of stream flow for the optimum use of water supplies and the prevention of flooding. The portion of precipitated water that can be stored in the near surface zone depends on the characteristics of the surface soil conditions (e.g., the amount of moisture in the soil) before the storm began and how much rain would have to fall before saturation will occur. In agricultural fields, knowledge of the moisture content in near surface layers can be used to monitor the growth of plants in their early stages. In addition, remotely sensed soil moisture data could aid in gaining a greater insight into the mechanisms (e.g., evapotranspiration) which affect moisture flux from the ground surface to the atmosphere, a critical input for understanding the total global hydrologic cycle.

The objectives of this experiment were to assess the performance of an L-band, 25 cm wavelength imaging radar for soil moisture determination and to study the temporal variability of radar returns from a number of agricultural fields.

Several other experiments were conducted to remotely determine the soil moisture content by imaging radar technique. This experiment is the first designed to minimize the effects of vegetation cover and surface roughness on the radar return by repetitive measurements over the test fields.

The experiment, sponsored by the National Aeronautics and Space Administration (NASA) Goddard Space Flight Center, employed the Jet Propulsion Laboratory (JPL) L-band imaging synthetic aperture radar system in a series of overflights of an agricultural test site in Kern County, California (see Figure 1). Supporting field data were collected by the Geography Remote Sensing Unit (GRSU), University of California, Santa Barbara. Coincident aircraft and field verification data were obtained on March 24, 25, and 23, 1977. The L-band SAR system was flown onboard the NASA Ames Research Center (ARC) based CV-990 aircraft at an altitude of approximately 30,000 feet (9100 m). Data were obtained in both HH and HV polarization in an analog image format which were later converted to digital format for processing and analysis.

Following a brief background discussion of the research which has led to this study we will discuss the aircraft data acquisition and calibration phases of this experiment. This is followed by a discussion of the field verification procedures employed. Finally, an analysis of the resulting data from the combined aircraft and

RADAR SOIL MOISTURE STUDY AREA  
KERN COUNTY, CALIFORNIA

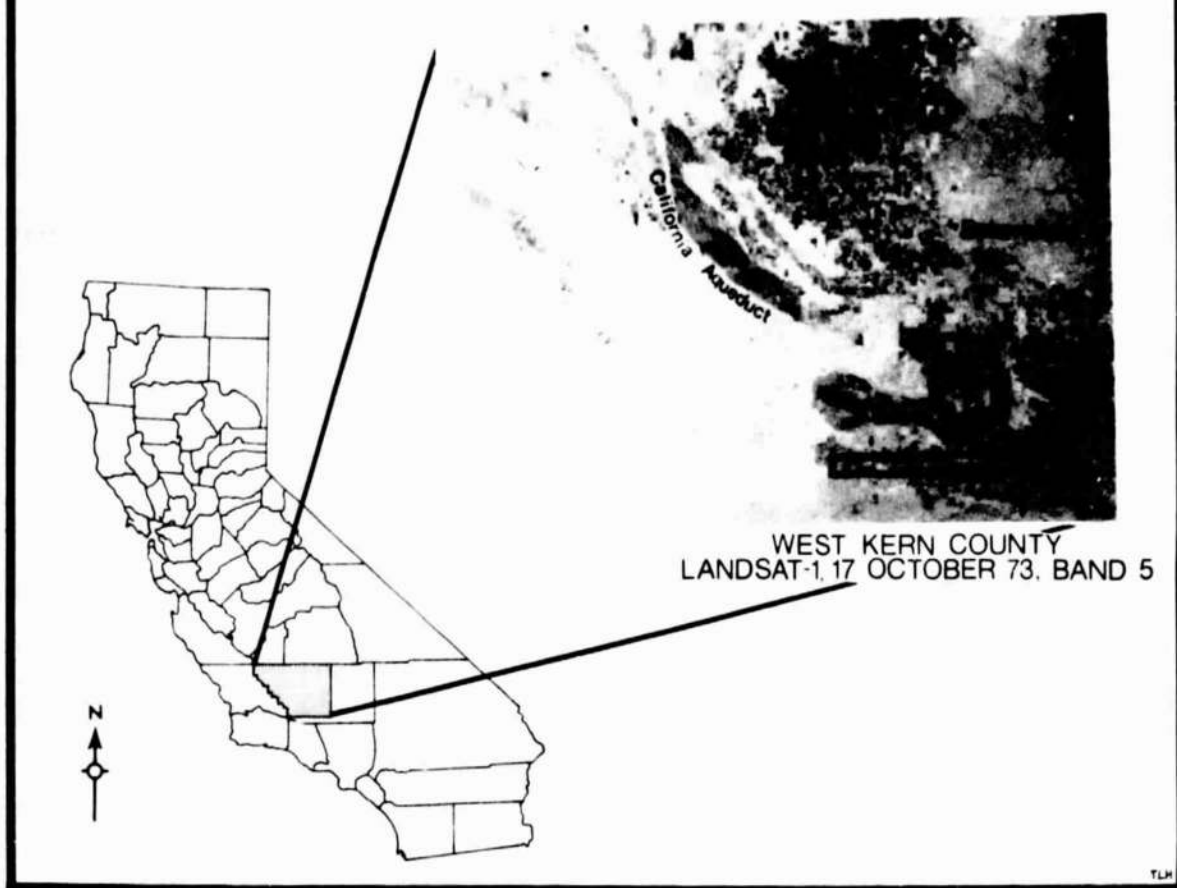


Figure 1. Copus Road Transect, Kern County, California

REPRODUCIBILITY OF THE  
ORIGINAL PAGE IS POOR

field data acquisition program leads into our conclusions that in this experiment the active microwave system employed demonstrated a responsiveness to soil moisture in the top 2 cm of fields free of vegetation.

BACKGROUND

Among the remote sensor systems being investigated for their ability to provide an accurate quantitative measurement of soil moisture in the surface to the root zones, active (radar) microwave systems are receiving considerable attention. The radar backscattering cross section for a soil has been studied extensively by using truck-mounted and air-borne scatterometers and spectrometers over agricultural fields (Batlivala and Ulaby, 1977, Ulaby and Dobson, 1977). These measurements have shown the sensitivity of radar return to soil moisture and other surface parameters such as surface roughness and vegetative cover. Recent airborne radar measurements (Blanchard, 1977 and Choudhury et al., 1978) show an encouraging relationship between the radar return and the soil moisture content. However, no definitive results have yet been reported from airborne radar systems.

Active microwave systems operating at longer wavelength demonstrated lower sensitivity to surface roughness and have a greater capability to sense moisture variation under a vegetative cover than those operating at shorter wavelengths (Batlivala and Ulaby, 1975, Batlivala and Dobson, 1976, Ulaby, et al., 1977). Conclusions derived from the measurements indicate that the instruments operating at longer wavelengths are preferable for the remote sensing of soil moisture.

AIRCRAFT DATA ACQUISITION AND CALIBRATION

During the Kern County soil moisture experiment the JPL L-band SAR collected multipolarized (HH and HV) data, on March 24, 25, and 28, 1977. This side looking SAR, chirped downward between 1235 MHz and 1215 MHz and has a ground resolution of approximately 20 m. Given the radar system delay of 105 msec., and the altitude of 30,000 feet, the resulting radar image has a swath width of approximately 8 km. The radar image, essentially a two-dimensional representation of the backscatter (reflection) cross section of the terrain exhibits, in its raw and unprocessed stage, some geometric distortion (Figure 2). As can be seen from this figure, the near range portion of the data ( $0^\circ$  to  $10^\circ$  incidence angle) is greatly compressed and is therefore of little value for either manual or automated analysis techniques. Thus, when this portion of the data has been removed, the resulting useable radar image represents a ground swath of approximately 6 km width. At the present time, there are no calibrated airborne imaging radar systems collecting data for earth resources analysis. By this it is meant

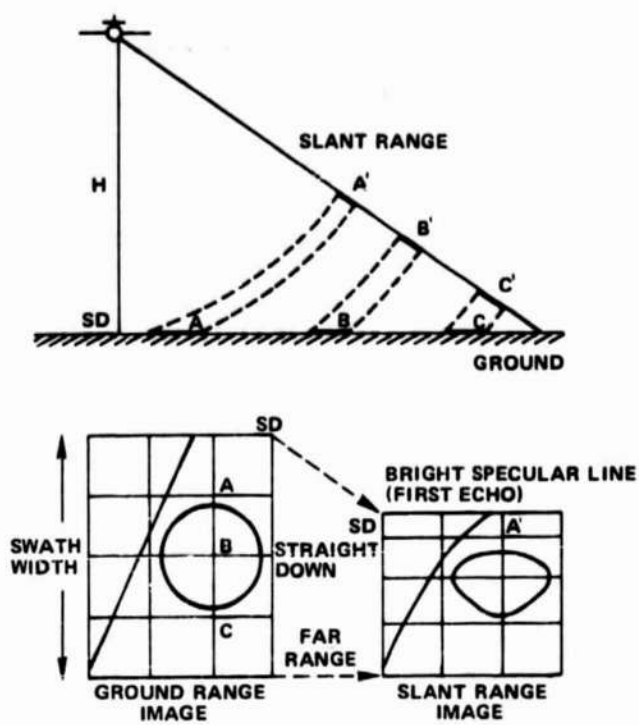


Figure 2. Slant Range Relationship for a SAR

that for no existing system acquiring for environmental applications are we able to determine the absolute backscatter cross section ( $\sigma^0$ ) of a given pixel. Even when the imagery, in the positive or negative transparency form, is digitized such absolute calibration is still not possible. Generally, for such calibration, it is common to pass the radar swath through a set of radar reflectors of known cross section and use these points for calibration points. This was not done here. Thus, for this study only relative radar return could be calculated. In addition, the processing configuration of data from this system limits acquisition of absolute return power information. The dynamic range of this radar is of the order of 50 dB and hence is much greater than that which can be preserved on a photographic image which is on the order of 15 dB. Thus we are severely limited in determining absolute return from the image data. Because the radar system used is a synthetic aperture radar, a signal film composed of a series of Doppler histories is recorded and optically correlated to produce the final image. It is at this stage when the correlated image is placed on the photographic film that the large dynamic range is lost. There are systems available to place the correlated image on a digital tape by scanning the correlator output rather than placing the image on a film. This would preserve most of the dynamic range of the radar but would still not yield the calibration which is required for detailed and reproducible work.

In this study we have attempted to minimize these problems in the most appropriate manner given the resources available. This was done by flying the system on three different days using the same flight tracks and radar system parameters. Noise power was then inserted into the L-band receiver at nine levels (in 5 dB steps between -95 dB and -55 dB) and recorded on the signal film at the beginning and end of each of the data runs. These noise power wedges were then correlated, along with the image signal and scanned along with the radar images. The scanning of the image transparency produced by the normal optical correlation of the signal film, was conducted on a Perkin-Elmer PDS Series 1000C microdensitometer with an azimuth and range aperture of  $20 \mu\text{m}$  and an azimuth and range spacing of  $20 \mu\text{m}$ . By comparing the wedge data number and the image data number, as recorded on the digital tapes, it is possible to convert the image data number into receive power. This methodology is particularly useful in linearizing the radar data and in calculating the relative backscatter coefficient. Following scanning, the levels were averaged and filtered to produce a set of relatively smooth curves in the range direction (Figures 3 through 5). In these figures, parts "A" are plots of the data number versus dB power for range time delay at five microsecond time integrals. On part "B" of these figures the x-axis is the range time delay (in microseconds) whereas the y-axis is the data number of the noise wedge in each corresponding 5 dB step.

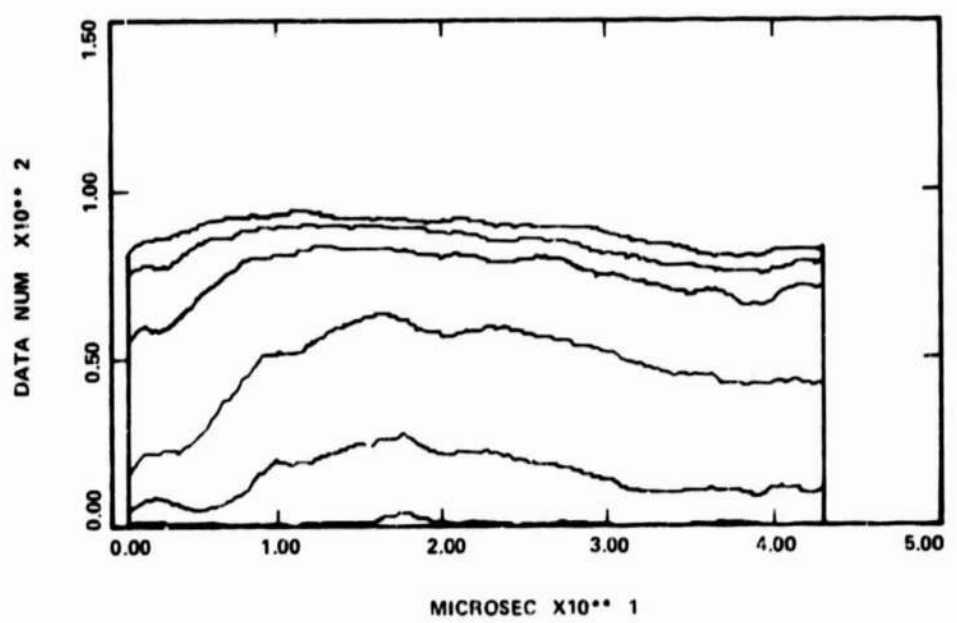
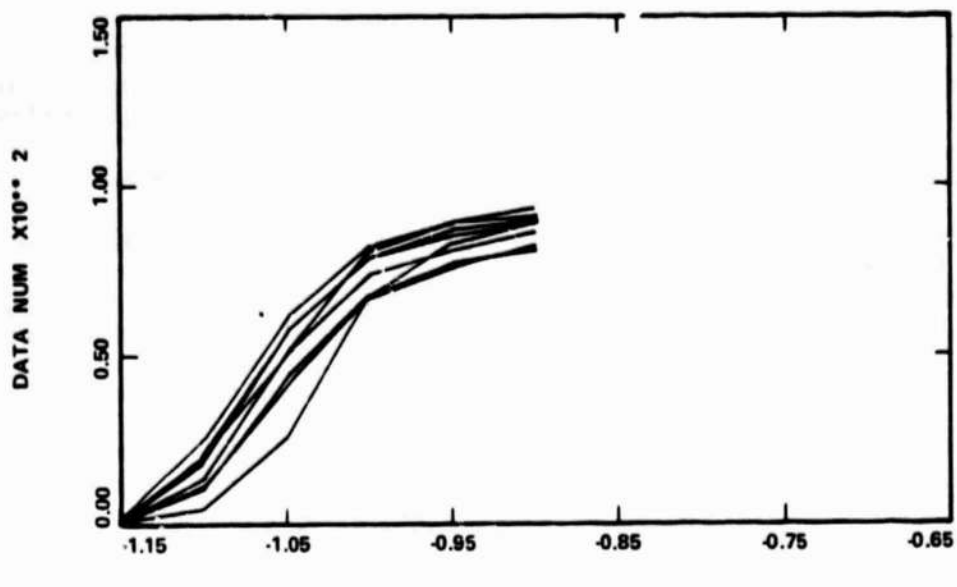


Figure 3. Calibration Data for March 24, 1977 Flight

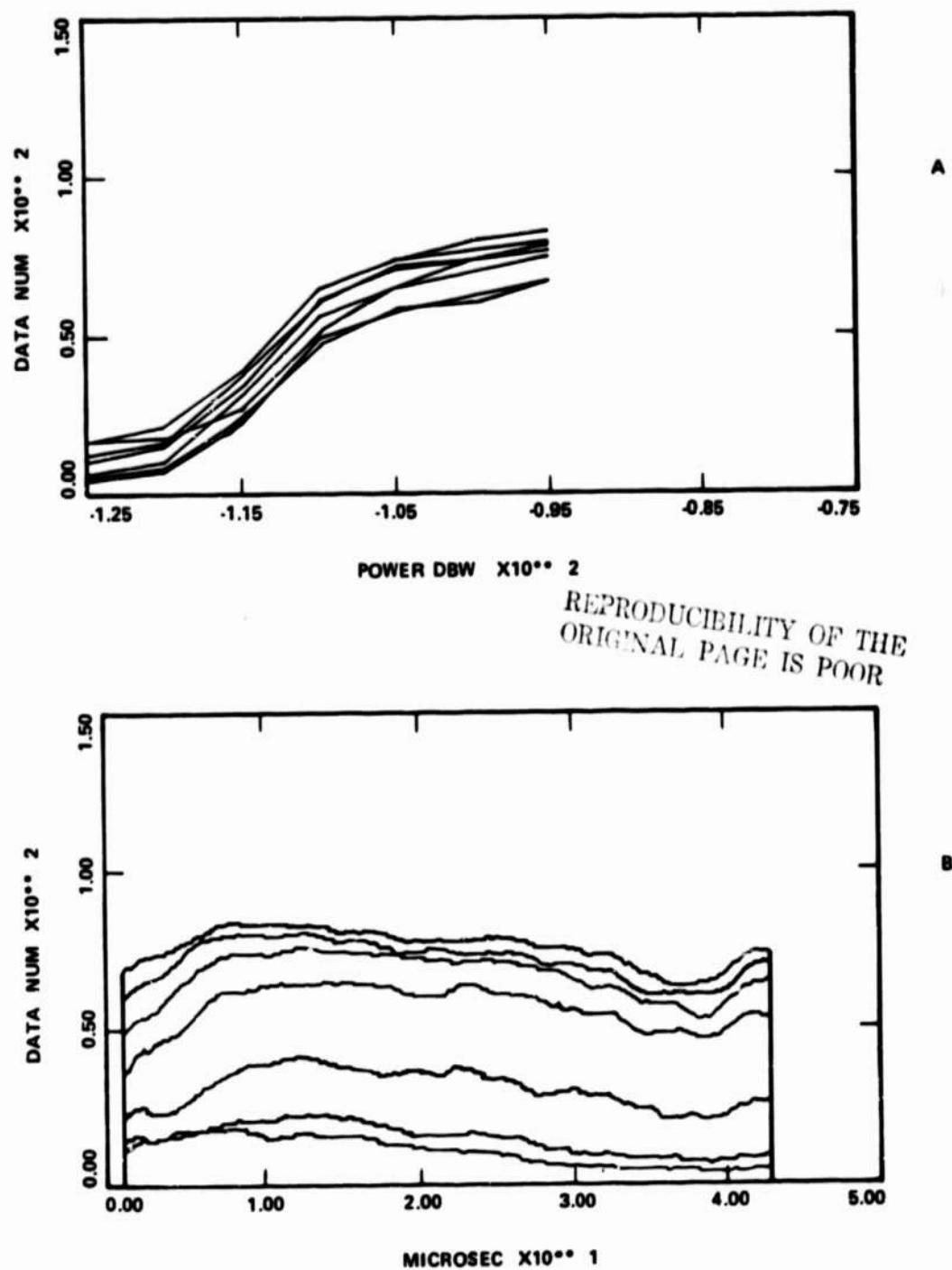


Figure 4. Calibration Data for March 25, 1977 Flight

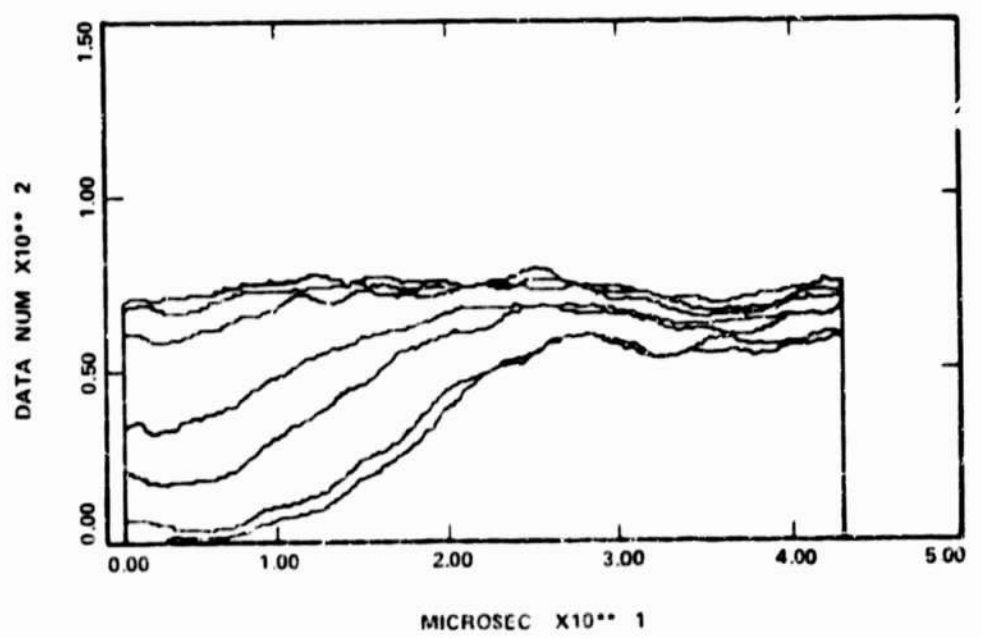
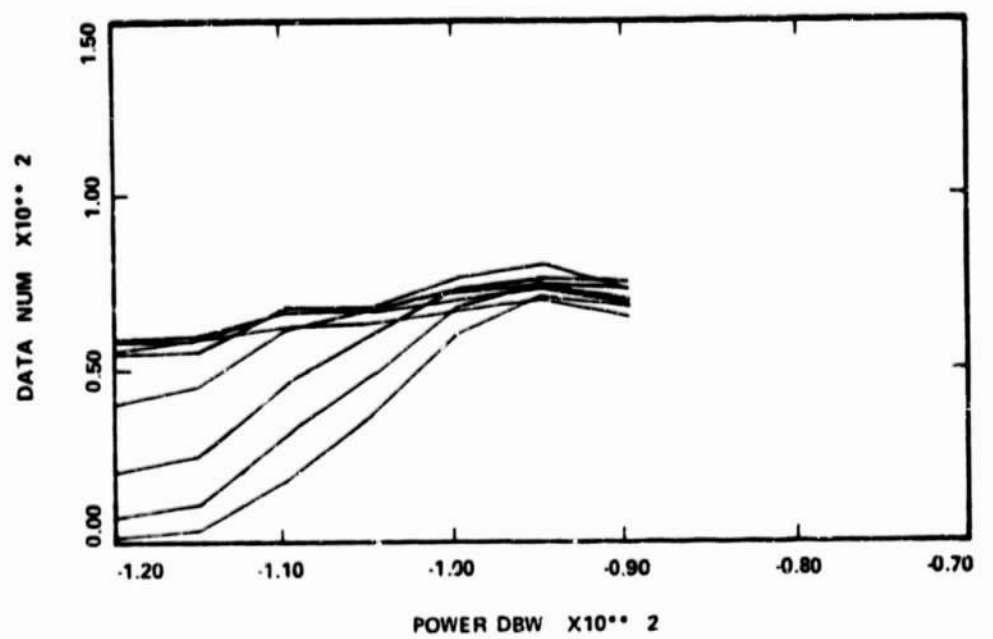


Figure 5. Calibration Data for March 28, 1977 Flight

The noise power wedges are then stored as a power interpolation table for each range data location for each data run. The data number from the scanned radar images is compared with the data number of the several power levels for corresponding range locations and the received dB power is then calculated as a linear interpolation between the noise wedges. The actual received power can then be obtained by converting the dB power number to power. Thus, it is possible to convert the entire radar image to power received using the noise power wedges. Errors due to film processing a similar (but unknown) transfer functions are thus minimized because the noise power wedges go through the same transfer functions as do the radar images.

By then using this received power as determined by the noise power wedges inserted into the signal film prior to and directly following each data run, it is possible to estimate the relative backscatter coefficient for the returned signal. The procedure used in calculation of the backscatter coefficient is given below. Equation (1) is the radar equation where  $P_r$  is power received,  $P_t$  is the transmitted power,  $G$  is the antenna gain,  $R_s$  is the slant range,  $\sigma_o$  is the backscatter coefficient,  $A_s$  is the ground surface area, and  $A_a$  is the effective antenna area.

$$P_r = \frac{P_t G}{4\pi R_s^2} \sigma_o A_s \frac{A_a}{4\pi R_s^2} \quad (1)$$

The effective antenna area is given by:

$$A_a = \frac{G\lambda^2}{4\pi} \quad (2)$$

where  $\lambda$  is the wavelength of the transmitted signal. The ground surface area is given by:

$$A_s = \frac{T C}{2 \tan \theta} R_s \theta_b \quad (3)$$

where  $T$  is the pulse duration,  $C$  is the speed of light,  $\theta$  is the angle from nadir and  $\theta_b$  is the effective azimuth beamwidth. Substituting the equations for the antenna and surface areas into equation (1) gives:

$$P_r = P_t \frac{G^2 \lambda^2}{(4\pi R_s)^3} T \frac{C}{2} \frac{1}{\sin \theta} \theta_b \sigma_o \quad (4)$$

The range R can be expressed as a function of altitude H and the angle from nadir;

$$R = \frac{H}{\cos \theta} \quad (5)$$

The antenna gain function for the L-band radar antenna is given by:

$$G = 15.8 \cos^2(\theta - 45^\circ) \quad (6)$$

Substituting the expressions for the range and the gain into equation (4) and solving for  $\sigma_0$  gives;

$$\sigma_0 = \frac{2(4\pi H)^3}{P_t \lambda^2 T C \theta_b (15.8)^2} f(\theta) P_r \quad (7)$$

where:

$$f(\theta) = \frac{\sin \theta}{\{\cos^3 \theta \cos^4 (\theta - 45^\circ)\}^2} \quad (8)$$

The backscatter coefficient  $\sigma_0$  can be calculated from equation (7) using the following L-band radar parameters:

$$P_t = 4.3 \times 10^3 \text{ watts}$$

$$\lambda = 0.25 \text{ meters}$$

$$T = 1.25 \times 10^{-6} \text{ seconds}$$

$$\theta_b = 18^\circ = 0.3142 \text{ radians}$$

Altitude is given in flight logs,  $\theta$  is calculated from the range time delay by equation (9) where  $\tau$  is the range time delay from nadir and  $P_r$  is calculated using the noise power wedges and the scanned radar images.

$$\theta = \cos^{-1} \frac{2H}{C_\tau + 2H} \quad (9)$$

## REPRODUCIBILITY OF THE ORIGINAL PAGE IS POOR

The resultant data can then be played back to give geometrically corrected images of the estimated backscatter coefficient. Examples of final images are given in Figures 6 to 8.

In order to convert the digital data to relative return power (dBw), a calibration equation was derived by linear regression of the noise power wedge collected during the three data flights. In this experiment, most of the sampled fields were located between 15° and 25° radar incidence angle. Therefore, only the results with incidence angle near 20° were shown in Figure 9. The linear equation is:

$$P(\text{dBw}) = 0.34X(\text{CNT}) - 119.6 \quad (10)$$

with  $R^2 = 0.83$ . The standard deviation of the calibration signals is 10.34 dBw and the estimated error is 4.40 dBw.

### FIELD VERIFICATION

The field sampling design employed in this experiment was designed to test the ability of the L-band system to detect moisture in non-vegetated fields with furrows parallel to the radar beam and with homogenous soil types. We attempted to optimize flight scheduling and the selection of a test transect in an area of irrigated agriculture for a temporal range of data and a wide range of soil moisture variation. The results, although not providing a large temporal range of data (due to scheduling problems), did achieve a good range of moisture conditions due largely to the occurrence of precipitation during the experiment (average seasonal rainfall for the study area is less than 12.7 cm per year).

Fields were selected for sampling after preliminary field verification to establish their size, furrow direction and vegetative or crop conditions. Twelve test fields were selected. All fields were in a bare soil condition with eight furrowed in a north-south direction (parallel-to-the-beam) and four with no discernible tillage pattern. The latter were selected to ascertain the effect, if any, of row direction on signal return.

Field verification ("ground truth") data were collected in Kern County, California in an area of flat terrain along Copus Road. This area is known for its large field irrigated agriculture and areas of homogenous soil type. Sampled fields reflect this in their size, the average being 176 acres, and their soil type, for the most part, either fine loam or sandy clay loam.

Within-field soil moisture sampling was designed to obtain the largest number of moisture profiles per field, while maximizing the number of deep layer profiles (given time and resource limitations). Furrow patterns within individual fields required

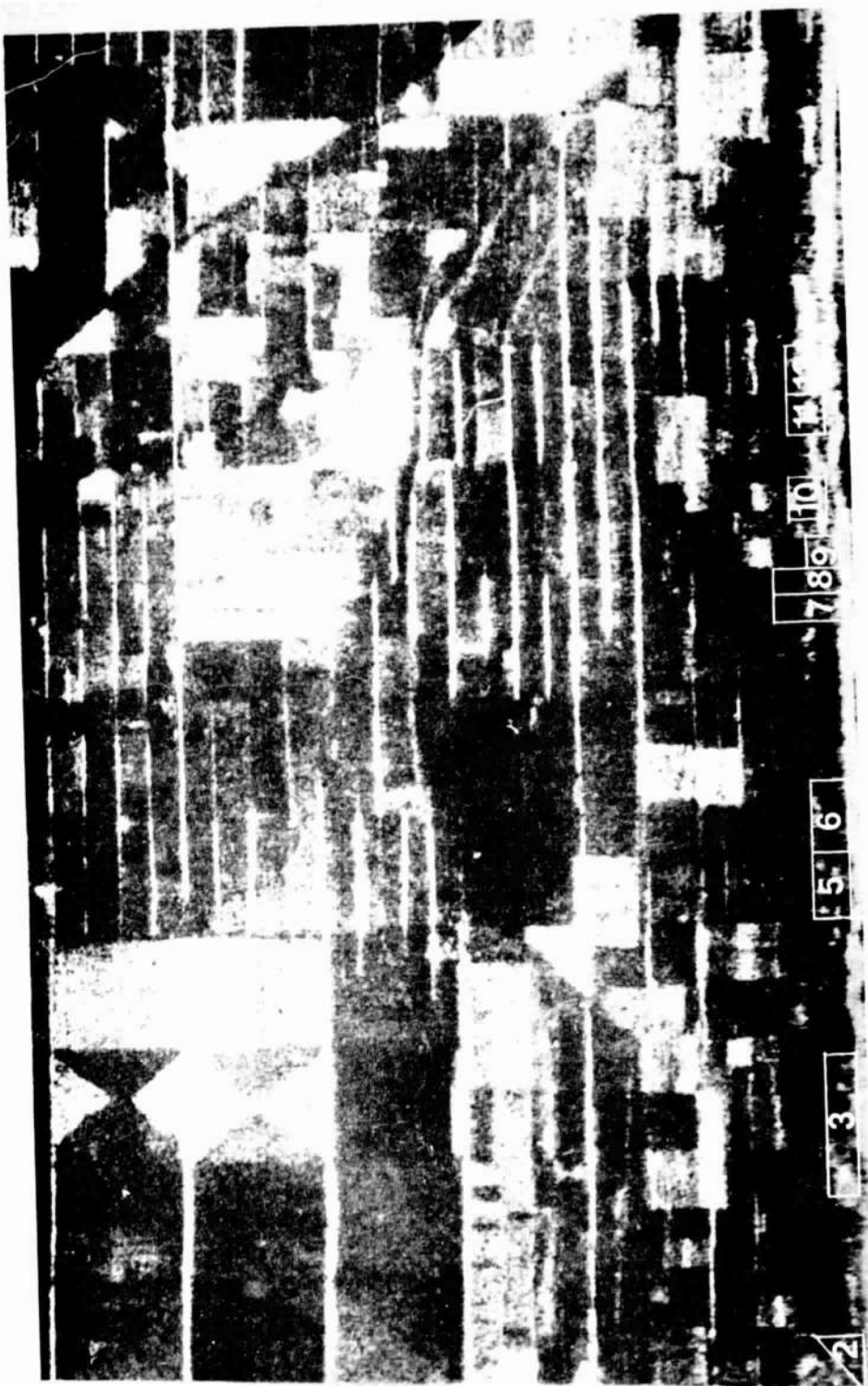
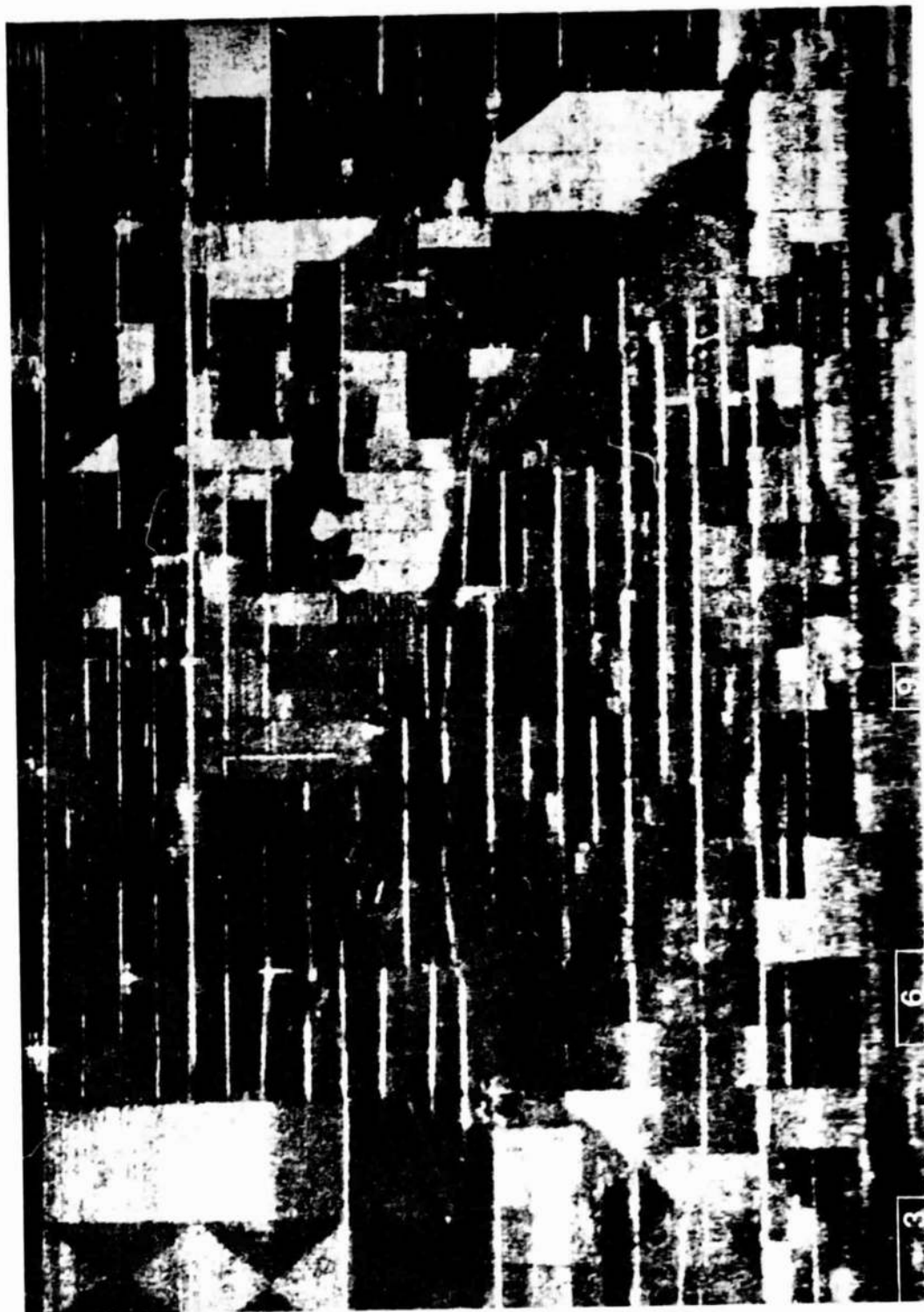


Figure 6. SAR Image for March 24, 1977 Flight

Figure 7. SAR Image for March 25, 1977 Flight



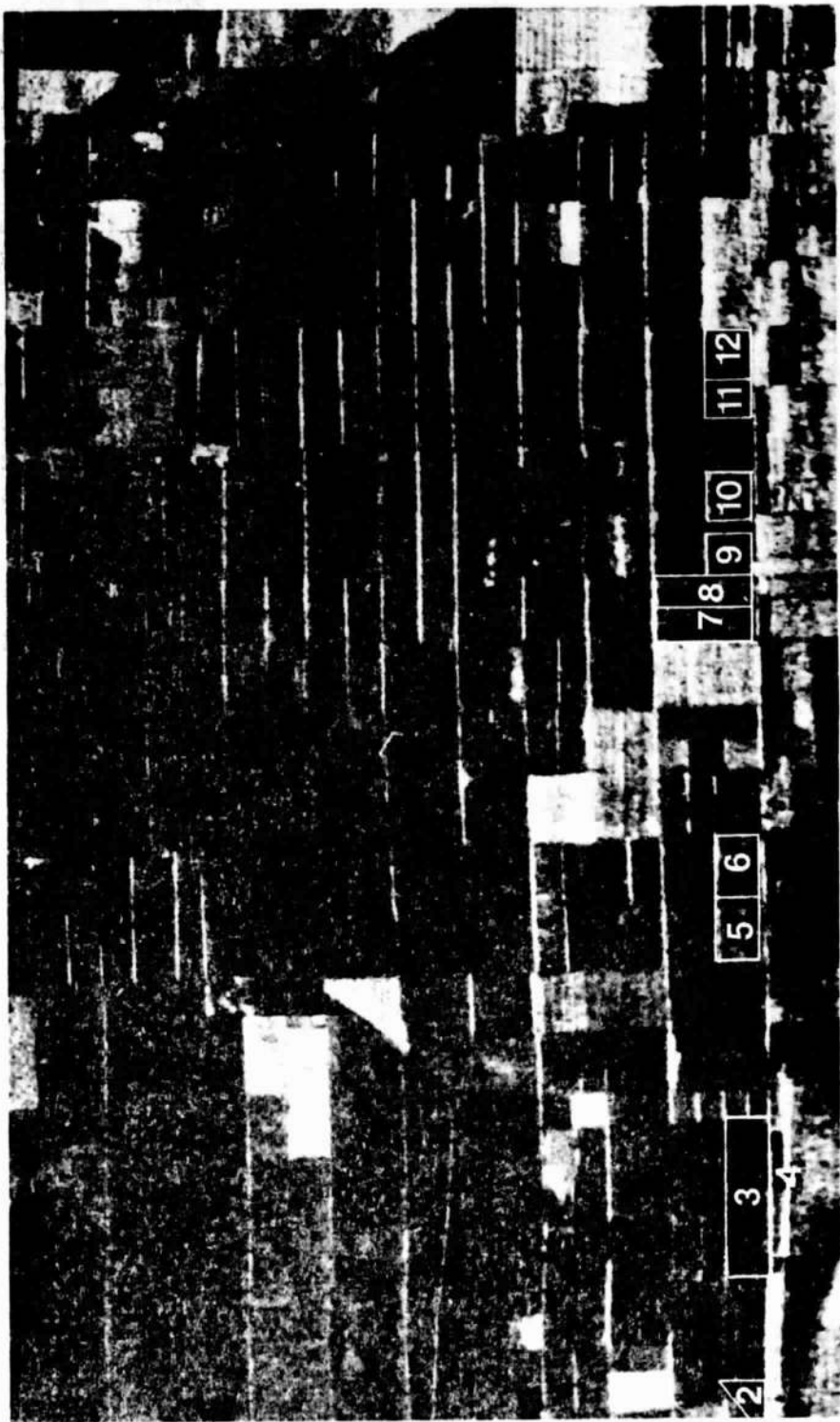


Figure 8. SAR Image for March 28, 1977 Flight

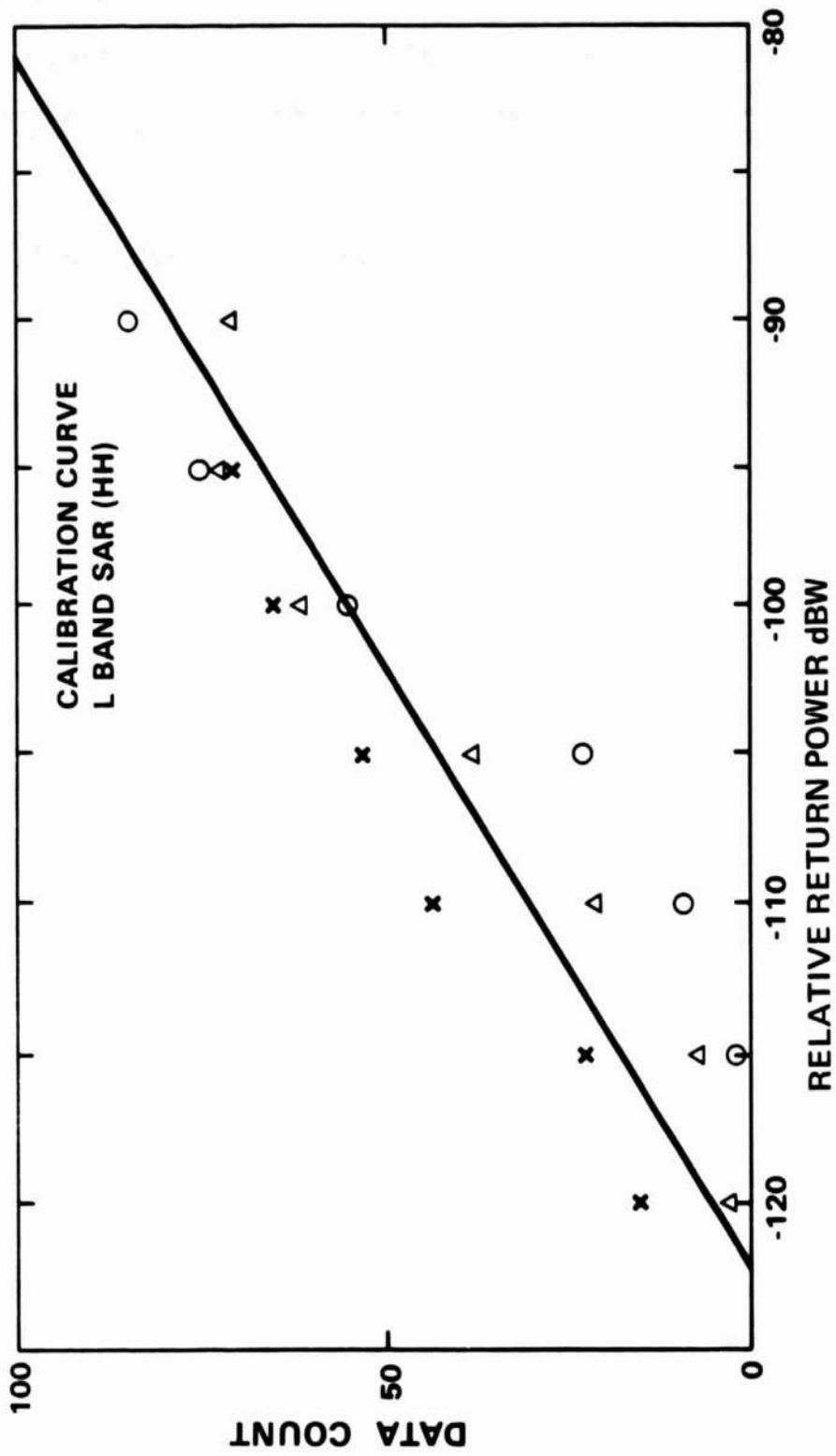


Figure 9. Calibration Curve for L-Band SAR (HH)

that separate profiles be taken from the top and bottom of each furrow due to expected moisture content differences. In each field soil profiles were obtained at nine separate sites, of which five were taken from the bottom of the furrow at 0-2, 2-5, 5-15, and 15-30 centimeter depths; and at the remaining four sites samples were taken from the top of the furrow at 0-2 and 2-5 centimeters.

The sampling design described above was used during the March 24 and 28, 1977 overflights. During the March 25, 1977 overflight it was necessary to revise the sampling because of a rainfall of 2.39 cm, (.94") just prior to the flight. This rainfall made the sandy clay loam of the test fields virtually impassable to field crews. In each field four profiles were taken from equally spaced locations approximately 15.2 meters (50 ft.) from the edge of Copus Road at depths of 0-5, 5-15, and 15-30 cm. In this design, the 0-2 and 2-5 cm depths were combined since the upper portion of the profile was saturated and essentially homogenous in terms of moisture. In field No. 12 only one profile was taken as the entire field was well saturated to below 30 cm.

Soil samples were taken directly to B.C. Laboratories\* in Bakersfield, some 40 kilometers from the test site, for processing. Each sample (soil plus tin) was weighed to a tenth of a gram and then placed in an oven at 105°C and reweighed at intervals until the difference between weighings was less than one tenth of a gram. This final dry weight was used to produce the gravimetric water content or percent soil moisture by weight (eq. 11):

$$\% \text{ of soil moisture} = \frac{\frac{\text{wet weight} - \text{dry weight}}{(\text{soil} + \text{tin})}}{\frac{\text{dry weight} - \text{tin weight}}{(\text{soil} + \text{tin})}} \times 100 \quad (11)$$

\*B.C Laboratories is certified by the California State Department of Health for chemical, bacteriological and bio assay, water, and waste analyses and has been performing agricultural, petroleum, construction and pollutant testing since 1949.

Using the formulas derived by Schmugge et al. (1976) and the soil fraction data obtained from samples taken in each test field, the values for field capacity and wilting point were calculated for each field. The values for percent moisture content by weight were then converted to percent of field capacity.

Field verification data were acquired as closely as possible to the time of the JPL aircraft overflights, usually between 12 pm and 5 pm with aircraft overflights typically occurring between 3 pm and 4 pm. Data collected for each field included:

- percent soil moisture by weight and percent of field capacity;
- furrow direction, height, width and soil clod size based on photographs taken against a 2" incremented grid set;
- soil texture;
- irrigation history for each field for the months of February and March;
- climatological data for each overflight consisting of average daily wind speed, relative humidity and cloud cover as well as the precipitation history for the area for the months of February and March taken from the National Weather Service station at Kern County Airport in Bakersfield;
- soil type information for the test site is taken from the U.S. Department of Agriculture Soil Survey Series 1937, No. 12 for the Bakersfield, California area.

Samples of the soil moisture and percent of field capacity data are shown in Tables I and II. Tables III and IV respectively give the field average percent moisture content by weight and the field average percent of field capacity.

#### Results and Analysis

To derive the SAR backscatter from bare soil fields, it was necessary to obtain the average data number within each sampled field boundary. In this study, these averages were obtained by using the Atmospheric and Oceanographic Information Processing System (AOIPS). This system produces a tone-contrast black and white visual image of the digital data numbers on a cathode ray tube. From the visual image, the field boundaries were identified for each field from which ground soil moisture measurements were taken. Built-in software within the AOIPS was used to calculate the mean and the standard deviation of each field. Subsequently, these field averages were converted to relative return power by equation (10). The results are tabulated in Table V. Due to the steep incidence angle of observation ( $15^\circ$ ) of some of these fields

and their subsequent locations in the very compressed portion of the radar image, it was difficult to resolve their field boundaries. Thus, Table V contains some missing values for relative return power.

Without precipitation during the previous week, the measured percent moisture content of field capacity (%FC) for bare/fields on March 24 was relatively dry,  $\approx$  15%FC for the top 0-2 cm soil samples. On March 25, about 2 cm of precipitation were recorded. Following the rain the average measured %FC that day was about 130%. Three days later, when the third flight took place, the 0-2 cm soil samples had dried considerably. Average %FC for fields sampled March 28 was  $\approx$  60%.

In examining all the available data, the radar return did not appear to correlate well with the measured soil moisture and percent field capacity. This was probably due to the combined effects of soil moisture content and surface roughness variations.

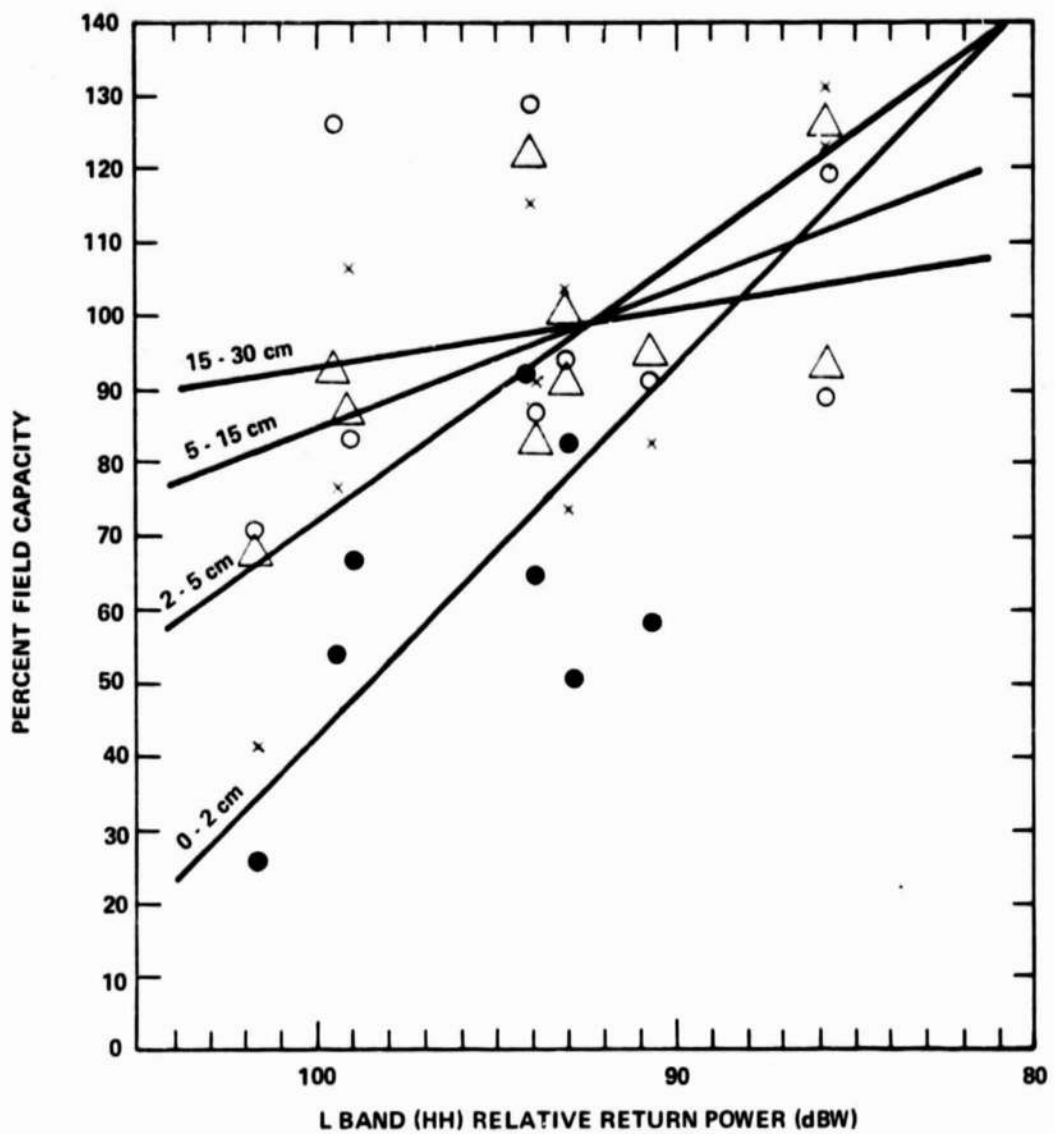
In order to separate the effects of soil moisture and surface roughness, the data were divided into two categories according to the field condition. They are (1) furrowed fields with maximum clod size 2.5 cm to 12.5 cm, including fields 1, 2, 3, 4, 9, 10, 11, and 12, and (2) unfurrowed fields with maximum clod size 15 cm to 20 cm, including fields 5, 6, 7, and 8. The furrowed fields were all oriented in a north-south direction which was parallel to the radar beam. The furrow width was approximately 100 cm and height is about 20 cm. The linear regression between the 0-2 cm %FC and the relative return power from furrowed fields is significant at the 1% level ( $r^2$  of 0.69). The estimated error of %FC is 19.4%. The regression equation is:

$$\text{%FC} = 537.64 + (4.95 \times P(\text{dBw})) \quad (12)$$

Figure 10 displays the relative return power from furrowed fields vs %FC. Although the estimated error for 0-2 cm %FC is quite large, it appears adequate to separate surface soil moisture conditions in dry, medium dry, and wet categories.

As can be seen in Figure 10 the relationship between return power and %FC becomes progressively weaker further into the soil profile. A similar regression between %FC in non-furrowed fields and power returned indicates no significant relationship at any of the sampled depths. This may be due to the highly irregular geometry of the surface in these fields which may override any effect soil moisture variations have on the radar signal.

Since the regression was carried out with samples for dry, mid and saturated states it indicates that extreme values, some 15 db apart, are likely to be detectable. Thus the passage of rainfall,



● 0 - 2 cm	$r^2 = .69$	$\%FC = 537.64 + (4.95 \times RRP)$
× 2 - 5 cm	$r^2 = .50$	
△ 5 - 15 cm	$r^2 = .37$	
○ 15 - 30 cm	$r^2 = .05$	

Figure 10. L-Band (HH) Relative Return Power vs Percent Field Capacity for Different Soil Layers

or recent irrigation should be readily detectable with calibrated radars. However, for the mid moisture ranges, even confining samples to those with similar roughness and a row direction parallel to the beam, it would be hard to argue from this small data set that a useable relation could be derived.

### CONCLUSIONS

Results from this experiment demonstrated that the return from imaging radar is responsive to the amount of soil moisture in the surface of bare fields where furrowing is parallel to the radar beam. The signal returned from dry (15%FC) and wet (130%FC) fields differs by about 15 dB. The signal from non-furrowed fields appears to be unresponsive to soil moisture differences. However, there are problems that need to be resolved before this technique can be used in an operational application. First, adequate calibration of the radar systems will be required so that meaningful comparisons can be made for multitemporal data sets. Accurate systems calibration insuring the comparability of data from area to area within a single flight and between different flights is a basic requirement, and is needed before SAR data can be utilized to operationally monitor either hydrological or agricultural parameters. Without such calibration the correlation of data from different dates, a critical parameter is establishing saturation trends required in both hydrologic and agricultural forecasting, is impossible to obtain in any operationally meaningful manner.

The effect of surface roughness needs to be determined before this technique can be used for soil moisture determination even with this repetitive measurement technique. In this experiment the surface roughness appears to mask differences in relative return power which are thought due to soil moisture variation. The results indicate this to be a more significant problem in non-furrowed rather than in fields with parallel to the radar beam furrowing. More study including a more thorough documentation of surface condition is required to fully evaluate surface roughness effects on backscatter and accurate documentation of moisture conditions.

REPRODUCIBILITY OF THE  
ORIGINAL PAGE IS POOR

REPRODUCIBILITY OF THE  
ORIGINAL PAGE IS POOR

Table I  
SOIL MOISTURE GROUND TRUTH - MARCH 1977

Date: 24 MARCH 1977		FIELD NUMBER: 1													
TIME OF SAMPLING: 1325															
PERCENT SOIL MOISTURE															
DEPTH	SITE														
	A	B*	C	D*	E	F*	G	H*	I						
0-2 CM	5.1	3.3	3.5	2.5	2.2	2.4	1.3	2.0	1.5						
0-5 CM	10.9	6.8	15.5	4.7	12.7	5.2	3.8	3.2	4.5						
5-15 CM	18.8		14.8		15.7		8.5		9.6						
15-30 CM	15.5		15.6		15.3		5.4		7.8						

AVERAGE PERCENT SOIL MOISTURE

DEPTH	FIELD AVERAGE TOP OF FURROW SITES B, D, F, H	FIELD AVERAGE BOTTOM OF FURROW SITES A, C, E, G, I	FIELD AVERAGE COMBINED ALL SITES
0-2 CM	2.5	2.7	2.6
2-5 CM	5.0	9.5	7.5
5-15 CM		13.5	13.5
15-30 CM		11.9	11.9

\*SAMPLES WERE TAKEN FROM THE TOP OF THE FURROW AND AT ALL OTHER LOCATIONS FROM THE BOTTOM OF THE FURROW

Table II  
SOIL MOISTURE OF GROUND TRUTH - MARCH 1977

DATE: 24 MARCH 1977	FIELD NUMBER: 1								
TIME OF SAMPLING: 1325									
PERCENT CLAY: 28.8									
PERCENT SAND: 33.2									
PERCENT SILT: 38.0									
FIELD CAPACITY: 24.5	WILTING POINT: 11.8								
PERCENT OF FIELD CAPACITY									
DEPTH	SITE								
	A	B*	C	D*	E	F*	G	H*	I
0-2 CM	20.8	13.5	14.3	10.2	9.0	9.8	5.3	8.2	6.1
2-5 CM	44.5	27.8	63.3	19.2	51.8	21.2	15.5	13.1	18.4
5-15 CM	76.7		60.4		64.1		34.7		39.2
15-30 CM	63.3		63.7		62.4		22.0		31.8

AVERAGE PERCENT OF FIELD CAPACITY

DEPTH	FIELD AVERAGE TOP OF FURROW SITES B, D, F, H	FIELD AVERAGE BOTTOM OF FURROW SITES A, C, E, G, I	FIELD AVERAGE COMBINED ALL SITES
0-2 CM	10.4	11.1	10.8
2-5 CM	20.3	38.7	30.5
5-15 CM		55.0	55.0
15-30 CM		48.7	48.7

\*SAMPLES WERE TAKEN FROM THE TOP OF THE FURROW AND AT ALL OTHER LOCATIONS FROM THE BOTTOM OF THE FURROW

Table III  
FIELD AVERAGE PERCENT MOISTURE CONTENT BY WEIGHT

DATE	DEPTH	FIELD									
		1	2	3	4	5	6	7	8	9	10
March 24, 1978	0-2 CM	2.6	2.6	6.1	4.5	1.6	1.9	2.1	2.2	13.7	5.9
	2-5 CM	7.5	9.6	9.5	10.3	4.5	6.5	4.4	5.2	17.1	9.5
	5-15 CM	13.5	12.4	15.9	16.0	8.4	9.6	9.4	10.9	20.9	13.2
	5-30 CM	11.9	10.3	16.0	12.2	7.7	9.2	9.4	9.0	22.9	11.8
March 25, 1978	0-5 CM	28.7	28.3			24.6			28.8		
	5-15 CM	23.5	23.3			23.9			27.5		
	15-30 CM	20.2	20.5			19.0			26.0		
March 28, 1978	0-2 CM	20.2	13.2	9.4	11.8	3.7	14.6	10.9	12.9	17.8	10.4
	2-5 CM	25.3	18.6	17.4	17.0	11.0	12.9	17.5	18.8	25.4	15.0
	5-15 CM	25.1	17.3	19.8	19.5	16.0	14.1	19.0	19.2	26.6	18.9
	15-30 CM	22.8	17.8	22.1	18.7	14.7	12.8	16.2	17.8	28.3	19.2

Table IV  
FIELD AVERAGE PERCENT OF FIELD CAPACITY

DATE	DEPTH	FIELD											
		1	2	3	4	5	6	7	8	9	10	11	12
March 24, 1977	0-2 CM	10.8	12.7	26.1	21.0	8.3	10.5	10.9	9.4	62.3	28.7	17.1	21.1
	2-5 CM	30.5	46.8	41.0	49.6	23.7	37.0	22.4	22.0	77.8	46.3	30.4	36.5
	5-15 CM	55.0	60.4	68.4	77.1	44.5	54.2	47.8	46.5	95.2	64.9	59.8	57.7
	5-30 CM	48.7	50.1	68.8	59.0	40.7	52.3	47.8	38.3	104.1	57.7	60.5	60.4
March 25, 1977	0-5 CM	139.2	122.0				140.0			130.6			
	5-15 CM	113.7	92.8				135.3			125.0			
	15-30 CM	195.4	88.2				107.5			118.2			
March 28, 1977	0-2 CM	82.5	64.0	40.4	57.2	20.1	82.1	55.7	55.2	91.2	50.7	66.3	53.5
	2-5 CM	103.1	90.5	75.1	82.0	58.9	73.1	89.4	80.4	115.2	73.5	106.2	76.1
	5-15 CM	102.4	83.9	85.5	94.1	84.3	80.3	96.7	82.2	121.0	92.7	85.8	92.4
	15-30 CM	93.1	86.3	95.2	90.1	77.7	72.8	82.9	76.1	128.5	93.9	82.8	126.2

Table V

Field averaged 0-2 cm percent moisture content, field capacity and SAR relative return power  
 (SM = % soil moisture, FC = % field capacity and RP = SAR relative return power in dBW)

Field Number	March 24			March 25			March 28		
	SM	FC	RP	SM	FC	RP	SM	FC	RP
1	2.6	10.8					20.2	82.5	-93.0
2	2.6	12.7		28.7	139.2		13.2	64.0	-93.8
3	6.1	26.1	-101.6	28.3	122.0	-85.7	9.4	40.4	
4	4.5	21.0					11.8	57.2	-90.6
5	1.6	8.3	- 89.2				3.7	20.1	-89.4
6	1.9	10.5	- 85.3	24.6	140.0	-90.1	14.6	82.1	-91.9
7	2.1	10.9					10.9	55.7	-91.7
8	2.2	9.4	-96.9				12.9	55.2	-90.3
9	13.7	62.3		28.8	130.6	-85.3	17.8	91.2	-93.9
10	5.9	28.7					10.4	50.7	-92.9
11	3.9	17.1					15.0	66.3	-99.0
12	4.5	21.1					11.4	53.5	-99.4

REPRODUCIBILITY OF THE  
 ORIGINAL PAGE IS POOR

## REFERENCES

1. Batlivala, P. P., and Ulaby, F. T., 1975. "Effects of Roughness on the Radar Response to Soil Moisture of Bare Ground." RSL Tech. Rpt. 264-5, University of Kansas Center for Research, Inc., Lawrence, Kansas.
2. Batlivala, P., and Dobson, C., 1976. "Soil Moisture Experiment (Kansas): Documentation of Radar Backscatter and Ground Truth Data." RSL 264-7, University of Kansas Center for Research, Inc., Lawrence, Kansas.
3. Batlivala, P. P., and Ulaby, F. T., 1977. "Feasibility of Monitoring Soil Moisture Using Active Microwave Remote Sensing." RSL Tech. Rpt. 264-12, University of Kansas Center for Research, Inc., Lawrence, Kansas.
4. Blanchard, B. J., June 1977. "Analysis of Synthetic Aperture Radar Imagery." Final Report RSC 2359-2, Texas A&M University, College Station, Texas.
5. Brown, W. E. Jr., Thompson, T. W., and Killpack, T., 1977. "Signal-to-Noise Ratio versus Wave Detectability." Pasadena, California, JPL Memo. Dated December 15, 1976, Revised January 12, 1977.
6. Choudhury, B. J., Chang, A. T. C., Salomonson, V. V., Schmugge, T. J., and Wang, J. R., 1978. "Preliminary Results of SAR Soil Moisture Experiment, November 1975." NASA TP-1404.
7. Schmugge, T., Wilheit, T., Webster, W. Jr., and Cloersen, P., 1976. "Remote Sensing of Soil Moisture with Microwave Radiometers-II." NASA Tech. Note TN-D-8321.
8. Ulaby, F. T., Bradley, G. A., Dobson, M. C., and Bare, J. E., 1977. "Analysis of the Active Microwave Response to Soil Moisture, Part II: Vegetation-Covered Ground." RSL Tech. Rpt. 264-19, University of Kansas Center for Research, Inc., Lawrence, Kansas.
9. Ulaby, F. T., and Dobson, M. C., 1977. "Analysis of the Active Microwave Response to Soil Moisture, Part I: Bare Ground." RSL Tech. Rpt. 264-18, University of Kansas Center for Research, Inc., Lawrence, Kansas.

## ACKNOWLEDGEMENTS

This paper presents the results of one phase of research carried out at JPL, California Institute of Technology, under contract NAS7-100, sponsored by the National Aeronautics and Space Administration. The authors wish to thank T. Killpack for his preparation of the estimated backscatter coefficients and W.T.K. Johnson for his review of the radar equations.

## BIBLIOGRAPHIC DATA SHEET

1. Report No.	2. Government Accession No.		3. Recipient's Catalog No.	
TM 80628				
4. Title and Subtitle L-Band Radar Sensing of Soil Moisture		5. Report Date 1980		
		6. Performing Organization Code 910		
7. Author(s) A.T.C. Chang et al.			8. Performing Organization Report No.	
9. Performing Organization Name and Address Goddard Space Flight Center Greenbelt Maryland 20771			10. Work Unit No.	
			11. Contract or Grant No.	
			13. Type of Report and Period Covered	
12. Sponsoring Agency Name and Address National Aeronautics and Space Administration Washington D.C. 20546			14. Sponsoring Agency Code	
15. Supplementary Notes				
16. Abstract The objectives of this experiment were to assess the performance of an L-band, 25 cm wavelength imaging synthetic aperture radar for soil moisture determination, and to study the temporal variability of radar returns from a number of agricultural fields. A series of three overflights was accomplished during March 1977 over an agricultural test site in Kern County, California. Soil moisture samples were collected from bare fields at nine sites at depths of 0-2, 2-5, 5-15, and 15-30 cm. These gravimetric measurements were converted to percent of field capacity for correlation to the radar return signal. Results of correlations between the relative return power and percent of field capacity (FC) demonstrate that the relative return power from this imaging radar system is responsive to the amount of soil moisture in bare fields. The signal returned from dry (15% FC) and wet (130% FC) fields where furrowing is parallel to the radar beam differs by about 10 dB.				
17. Key Words (Selected by Author(s))		18. Distribution Statement		
19. Security Classif. (of this report)		20. Security Classif. (of this page)		21. No. of Pages
				22. Price*